Catal Lett (2012) 142:601–607
DOI 10.1007/s10562-011-0752-6

Brønsted–Evans–Polanyi Relations for H_2O_2 Synthesis on Gold Surfaces

Yao-guang Wang · Jian-guo Wang

Received: 20 September 2011 / Accepted: 30 November 2011 / Published online: 27 March 2012
© Springer Science+Business Media, LLC 2012

Abstract By means of density functional theory calculations, the reaction mechanisms of H_2O_2 synthesis on three low index and two stepped Au surfaces have been investigated in detail. This study shows the activation energies of five elementary reaction steps of H_2O_2 synthesis, which include two hydrogenation and three decomposition steps of key species, are a function of reaction energies, which observe the Brønsted–Evans–Polanyi rules on both the flat Au surfaces and the step edge sites of stepped Au surfaces. This study not only provides a simple method to estimate the reaction barriers of elementary steps of H_2O_2 synthesis by the reaction energies but also predicts the catalytic performances of Au nanoparticles applied in real catalysis.

Keywords Brønsted–Evans–Polanyi relationship · AuPd surface · H_2O_2 · DFT

1 Introduction

H_2O_2, as an environmentally friendly oxidant, has played a large role in chemical industry [1, 2]. Direct synthesis of H_2O_2 from hydrogen and oxygen will certainly play an increasing important role in green chemical synthesis in which the formed H_2O_2 is directly applied in an oxidation reaction. Pd is the most widely investigated and highly efficient catalyst in the direct synthesis of H_2O_2 [3]. However, the low selectivity for H_2O_2 and harsh work conditions by using a mixture of H_2 and O_2 in concentration within the explosive range are the serious problems of Pd catalysts [4]. Gold catalysts have attracted special attention in the direct synthesis of H_2O_2 due to the extraordinary catalytic properties in a series of oxidation or selective oxidation reactions [5–11]. But monometallic Au catalysts supported on carbon or metal oxides show very little activity for H_2O_2 synthesis [3]. The study of Hutching and other research groups has shown that bimetallic catalysts, especially AuPd, have remarkable enhanced catalytic activity and selectivity in the direct H_2O_2 synthesis when compared with that of monometallic Au or Pd catalysts [3, 12, 13]. Recently, Hutchings has reported that nitric-acid pretreated AuPd catalyst supported on carbon gives high yields of H_2O_2 with hydrogen selectivities greater than 95% [14]. Particle size, atomic/surface compositions, the shape and exposed facets of nanocatalysts particles are all the influent factors of catalytic performances of AuPd [15–17]. Recently, these isolated Pd atoms within the gold matrix are indentified as the most active catalytic center for vinyl-acetate synthesis and the direct H_2O_2 synthesis reaction [18–21]. It is shown that single Pd sites enhanced H_2O_2 selectivity, whereas surface ensembles of contiguous Pd atoms support H_2O formation [21].

Independent of the used catalysts, during the direct H_2O_2 synthesis, the competing reaction channel is the formation of H_2O by the non-selective oxidation. The elementary reactions of H_2O_2 formation by the hydrogenation of molecular oxygen are as follows:

$$O_2 \rightarrow O_2{}^* \quad (1)$$

$$O_2^* + H^* \rightarrow OOH^* \quad (2)$$

$$OOH^* + H^* \rightarrow H_2O_2{}^* \quad (3)$$

$$H_2O_2{}^* \rightarrow H_2O_2(g) \quad (4)$$

It is seen that molecular oxygen (O_2), hydroperoxo (OOH) and hydrogen peroxide (H_2O_2) are three key

Y. Wang · J. Wang (✉)
College of Chemical Engineering and Materials Science, Zhejiang University of Technology, Hangzhou 310032, China
e-mail: jgw@zjut.edu.cn

species for H_2O_2 synthesis. Once these key species decomposition (reactions 5–7), the H_2O is easily formed.

$$O_2^* \rightarrow 2O^* \quad (5)$$

$$OOH^* \rightarrow O^* + OH^* \quad (6)$$

$$H_2O_2^* \rightarrow OH^* + OH^* \quad (7)$$

Therefore, the ideal catalysts should have high (low) activity for the H_2O_2 (1–4) (H_2O) formation (5–7) by the modulation of the geometric and/or electronic properties of nanocatalysts particles. The high resolution transmission electron microscopy characterization shows that Au or AuPd particles are dominated by (111), (100) facets, few (110) facets with different shapes of truncated octahedral, icosahedra and decahedra [22–24]. The exposed facet is one of major factors to determine catalytic properties of Au or AuPd particles. There are several theoretical studies [20, 25–32] of H_2O_2 synthesis on low index Pd, Au, Pt surfaces or small Au clusters. However, a systematically comparative study of the key elementary reactions for H_2O_2 and H_2O formation on these low index Au surfaces, especially Au(111), Au(100) and Au(110) and stepped Au surfaces, is very necessary.

In this study, by means of density functional theory (DFT) calculations, we investigate the formation and decomposition of three key species (O_2, OOH and H_2O_2) during H_2O_2 synthesis on three kinds of low index Au surfaces (Au(111), Au(100), Au(110)), which are the major facets of gold nanoparticles, and two stepped Au surfaces (Au(221) and Au(211). Our study shows that, on most of Au surfaces, reaction barriers of the formation of key intermediates are larger than those of their decomposition. Especially, we find that the activation energies of these reactions are a function of the reactions energies, which is consistent with the Brønsted–Evans–Polanyi rules [33, 34]. This rule provides a simple way to estimate the activation energies of H_2O_2 synthesis on Au surfaces and nanoparticles, which might be helpful to design novel Au nanocatalysts with superior activity and high selectivity.

2 Computational Details

The first principle DFT calculations were performed using the Dmol^3 program [35, 36]. The generalized gradient approximation (GGA) with the revised Perdew–Burke–Ernzerhof (RPBE) functional [37] was used to describe the exchange–correlation (XC) effects. The descriptions of the valence states were obtained with the double numerical basis set augmented with polarization p-function (DNP) [35] which has a computational precision being comparable with the Gaussian split-valence basis set 6-31G**. In this study, TS searches were identified using linear synchronous transit/quadratic synchronous transit (LST/QST) methods [38]. The TS approximation obtained in that way was used to perform QST maximization. TS confirmation tool based on Nudged-Elastic Band (NEB) [39, 40] algorithm was applied, which has been well validated to find the TS structure and the minimum energy pathway.

Three low index (Au(111), Au(100) and Au(110)) and two stepped surfaces (Au(211), Au(211)), in which one Au atom is substituted by Pd, have been considered in this study. These surfaces are defined as Pd_1/Au(111), Pd_1/Au (100), Pd_1/Au(110), Pd_1/Au(221), Pd_1/Au(211), respectivelly. For Pd_1/Au(111), Pd_1/Au (100), Pd_1/Au(221) and Pd_1/Au(211), a four layer 3×3 surface unit cells, for Pd_1/Au(110), a five layer 3×3 surface unit cells were used for all calculations. During the optimization process, only the most bottom Au layer was kept fixed while the remaining layers of Au surfaces and the adsorbates were fully relaxed. The Brillouin zone integration was carried out with $4 \times 4 \times 1$ k-point sampling, where the convergence tolerance of energy was set to 1.0×10^{-5} Ha and the maximum force was 0.002 Ha/Å.

3 Results and Discussion

3.1 H_2O_2 Synthesis on Low Index Au Surfaces

In this study, we investigated the elementary reactions of the formation of H_2O_2 and decomposition of three key intermediates on three low index (Pd_1/Au(111), Pd_1/Au (100), Pd_1/Au(110)) and two stepped (Pd_1/Au(221), Pd_1/Au(211)) surfaces.

Figure 1 shows the potential energy diagrams of elementary reactions of H_2O_2 synthesis on Pd_1/Au(111) Pd_1/Au (100) Pd_1/Au(110) surfaces. O_2 does not adsorb on three kinds of Au surfaces by using RPBE, PW91, PBE functions. On Pd_1/Au(111) Pd_1/Au (100) Pd_1/Au(110) surfaces, O_2 has the moderate adsorption strength, which is dependent on the specific functional. The adsorption is thermodynamically favorable on three surfaces by using PW91 and PBE functional as shown in Table 1. After the adsorption of molecular oxygen, two successive hydrogenation steps are necessary for the synthesis of H_2O_2. The activation energies of the formation of hydroperoxide (reaction 2) and H_2O_2 (reaction 3) on Pd_1/Au(111) is 0.48 and 0.28 eV, respectively. However, the reaction barriers of these hydrogenation reactions on the other two low index surfaces (Pd_1/Au(100) and Pd_1/Au(110)) are much larger than those on Pd_1/Au(111). The reaction barrier of OOH and H_2O_2 formation on Pd_1/Au(100) is 0.53 and 0.67 eV, while 0.66 and 0.73 eV on Pd_1/Au(110), respectively. The distance between oxygen and hydrogen in transition state of OOH formation on Pd_1/Au(111) is slightly larger than those on other two surfaces(Pd_1/Au(100) and Pd_1/Au(110)), as shown in Fig. 2.

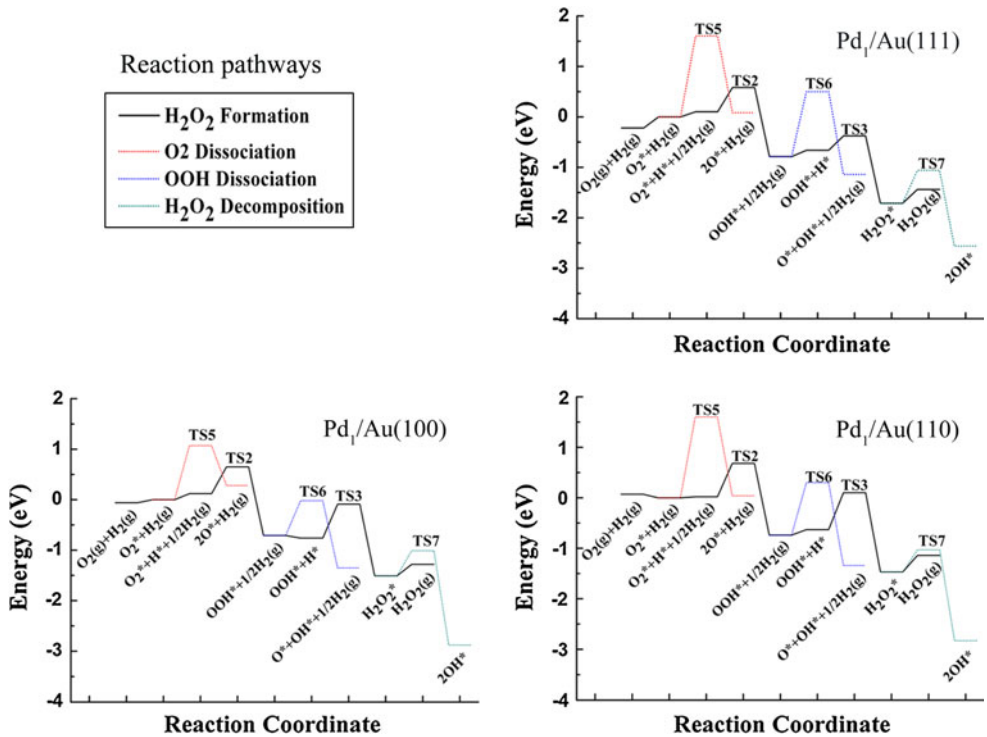

Fig. 1 Potential energy diagram for the elementary reaction (H_2O_2 formation (*black solid line*), O_2 dissociation (*red dot line*), OOH dissociation (*blue dot line*), H_2O_2 decomposition (*yellow dot line*) on three low-index surfaces

Table 1 The adsorption energy of O_2 calculated with different functions on five different Au surfaces

	RPBE	PW91	PBE
Pd_1/Au(111)	0.22	−0.17	−0.12
Pd_1/Au(100)	0.06	−0.38	−0.33
Pd_1/Au(110)	−0.07	−0.50	−0.45
Pd_1/Au(211)-st	−0.02	−0.45	−0.40
Pd_1/Au(221)-st	−0.05	−0.47	−0.42

Once the formation of H_2O_2, it easily desorbs from three Au surfaces. We also investigated the dissociation reactions of three key species for H_2O_2 formation. Among three low index surfaces, Pd_1/Au(100) is the easiest one to active O_2 and the corresponding activation energy is 1.07 eV. The reaction barriers of O_2 dissociation on Pd_1/Au(111) and Pd_1/Au(110) are both 1.60 eV, which is in agreement with the value (1.55 eV) reported by Hwang et al. [20]. Similarly, on Pd_1/Au(100), the dissociation of OOH into the adsorbed atomic oxygen and hydroxyl is also the easiest among three investigated surfaces. The activation energy of OOH dissociation on Pd_1/Au(100) is 0.69 eV, while it is 1.03 and 1.29 eV on Pd_1/Au(110) and Pd_1/Au(111) surfaces, respectively. The distance between oxygen and oxygen in transition states of OOH dissociation on Pd_1/Au(100) is much shorter than those on Pd_1/Au(110) and Pd_1/Au(111) surfaces (Fig. 2). However, Pd_1/Au(110) is the easiest one of three surfaces to

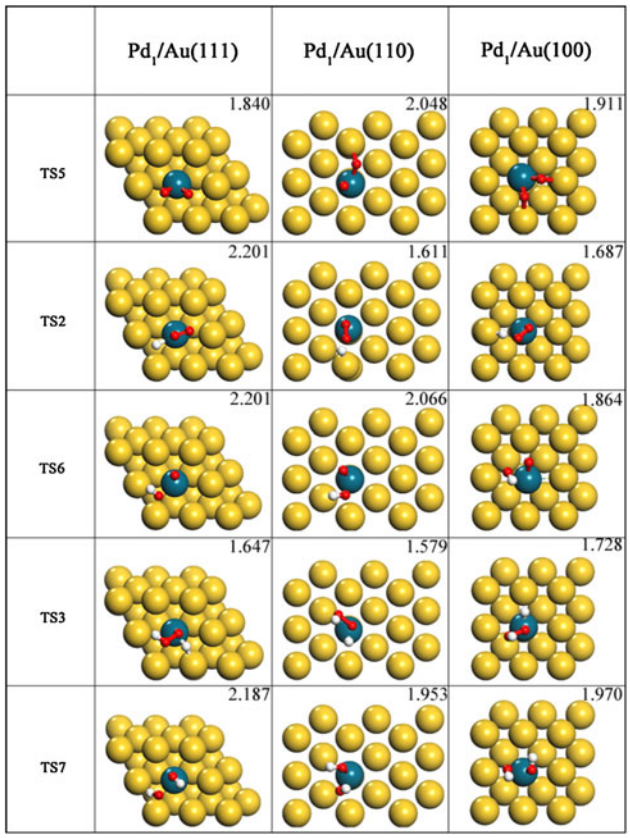

Fig. 2 The optimized transition states structures (*top view*) of the elementary steps on three low index surfaces. The bond lengths are given in angstrom (Å)

decompose H_2O_2 into two adsorbed hydroxyl, which needs to overcome a barrier of 0.44 eV. The H_2O_2 dissociation barrier on Au(111) and Au(100) is 0.65 and 0.50 eV, respectively. By comparing the reaction barriers of the hydrogenation and dissociation of key species on three kinds of surfaces, it is concluded that the hydrogenation of the relevant species are all easier than their dissociation.

3.2 H_2O_2 Synthesis on Stepped Au Surfaces

In order to simulate the edge sites of Au nanoparticles, two kinds of stepped Au surfaces (Pd_1/Au(221) and Pd_1/Au(211)), as the representative models, are used to investigate H_2O_2 reaction, as shown in Fig. 3. The Au(211) surface can be described as 3(111) × (100) in microfacet notation, a step-terrace structure consisting of three-atoms-wide of (111) orientation and a monatomic step with a (100) orientation. The Au(221) surface can be described as 4(111) × (111) in microfacet notation, a step-terrace structure consisting of four-atoms-wide of (111) orientation and a monatomic step with a (111) orientation. The Au(221) surface has a wider (111) terrace a lower density of step compared with the Au(211) surface. Further, two different substitutions of Au by Pd were considered, as shown in Fig. 3: the top of the step edge (1), and the terrace (2). On both Au (221) and Au (211) surfaces, the most favorable substitution site with one Pd atom is the terrace site. However, after O_2 adsorption, the Pd atom prefers the top of step edge by 0.09 eV for Pd_1/Au(221) and by 0.03 eV for Pd_1/Au(221). It is anticipated that the location of Pd on Au nanoparticles dynamically changes. All of elementary reactions on Au(111) are also investigated on two kinds of substituted Pd_1/Au(221) and Pd_1/Au(211) surfaces.

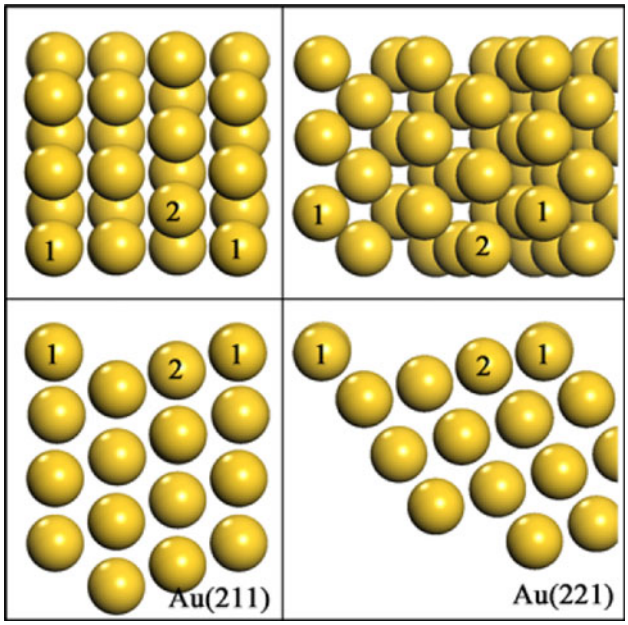

Fig. 3 Top view and side view of Au(211) and Au(221) surface. The substitution site is the step edge (*1*) and terrace (*2*), labeled as Pd_1/(211)-st, Pd_1/Au(221)-st and Pd_1/(211)-te and Pd_1/Au(221)-te, respectively

The adsorption energy of O_2 on the top of the step edge and the terrace site on Pd_1/Au(221) is -0.05 and 0.23 eV, respectively. On Pd_1/Au(211), the adsorption energy of O_2 also follows the same order, which are −0.02 and 0.22 eV on with RPBE functional, respectively (Table 1). Figure 4 shows the potential energy diagrams of elementary reactions of H_2O_2 synthesis on Pd_1/Au(221) and Pd_1/Au(211) surfaces. The reaction barriers of two hydrogenation steps on the top of step edge of Pd_1/Au(221) and Pd_1/Au(211) are much larger than those on Pd_1/Au(111) surface (Fig. 4). The smallest energy barrier of these hydrogenation reactions on the stepped surfaces is 0.66 eV, while the largest energy barrier of the hydrogenation reactions on the flat surface Pd_1/Au(111) is 0.48 eV. However, the reaction barriers of the competitive dissociation reactions on the top of step edge of Pd_1/Au(221) and Pd_1/Au(211) are smaller than those on Pd_1/Au(111) surface. Therefore, the step edge of Pd_1/Au(221) and Pd_1/Au(211) is much less favorable for H_2O_2 synthesis than the terrace site of Au(111). It is difficult to split O_2 on the terrace of Au(221) and Au(211) by the energy cost of 1.33 and 1.30 eV, respectively, which is slightly smaller than that on Pd_1/Au(111) surface. Similar with Pd_1/Au(111), the hydrogenation of O_2, OOH needs smaller energy than the dissociation of OOH and H_2O_2. For example, the reaction barriers for the formation of OOH and H_2O_2 on the terrace of Au(221) and Au(211) are all about 0.30 eV. However, the minimum energy to split OOH and H_2O_2 on the terrace of Au(221) and Au(211) is more than 0.70 eV. Therefore, our study shows that the reactivity of terrace sites of the stepped surfaces is very similar with the flat surfaces. Indeed, the transition state geometries on the terrace sites of the stepped surfaces are very similar with those on the flat surfaces (Fig. 5).

3.3 Brønsted–Evans–Polanyi relations of H_2O_2 Synthesis on Au Surfaces

In the above section, we analyzed the detailed reaction mechanism of H_2O_2 synthesis on three flat and two stepped Au surfaces. It is very important to seek one or a few descriptors to describe the catalytic performances. The Bronsted-Evans-Polanyi relations provide a nearly linear relationship between the activation and reaction energies of one elementary step. At present, the Brønsted–Evans–Polanyi relationships are mostly used in one or one type of bond dissociation or formation on different metal surfaces. To the best of our knowledge, very few reports on the Brønsted–Evans–Polanyi relationships for the complete

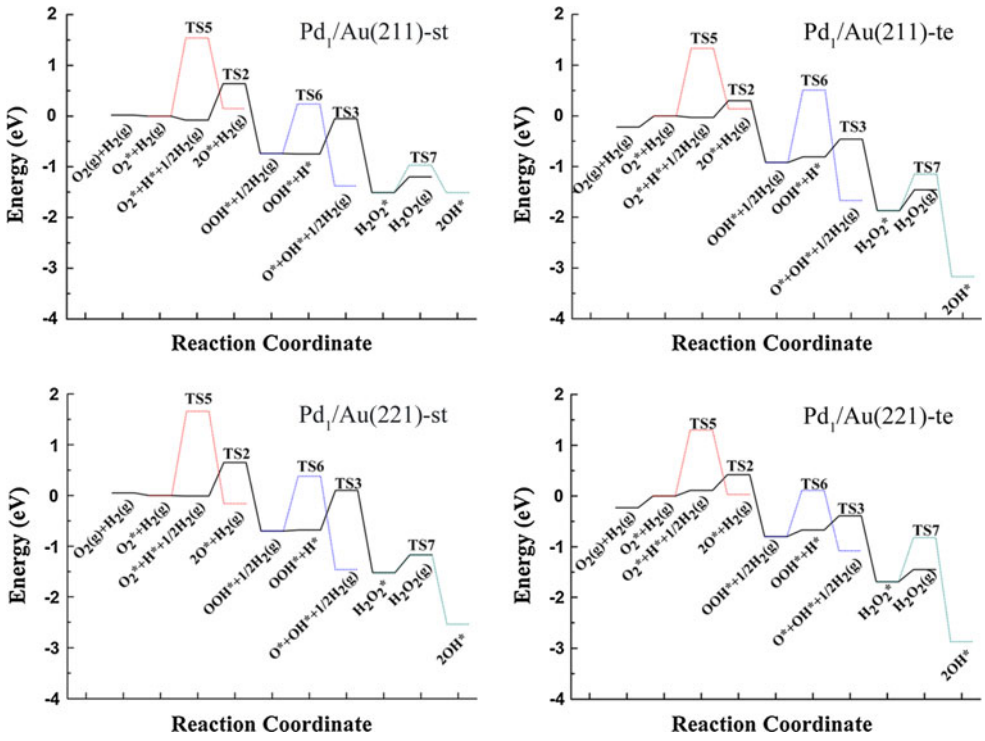

Fig. 4 Potential energy diagram for the elementary reaction (H_2O_2 formation (*black solid line*), O_2 dissociation (*red dot line*), OOH dissociation (*blue dot line*), H_2O_2 decomposition (*yellow dot line*)) on two stepped surfaces

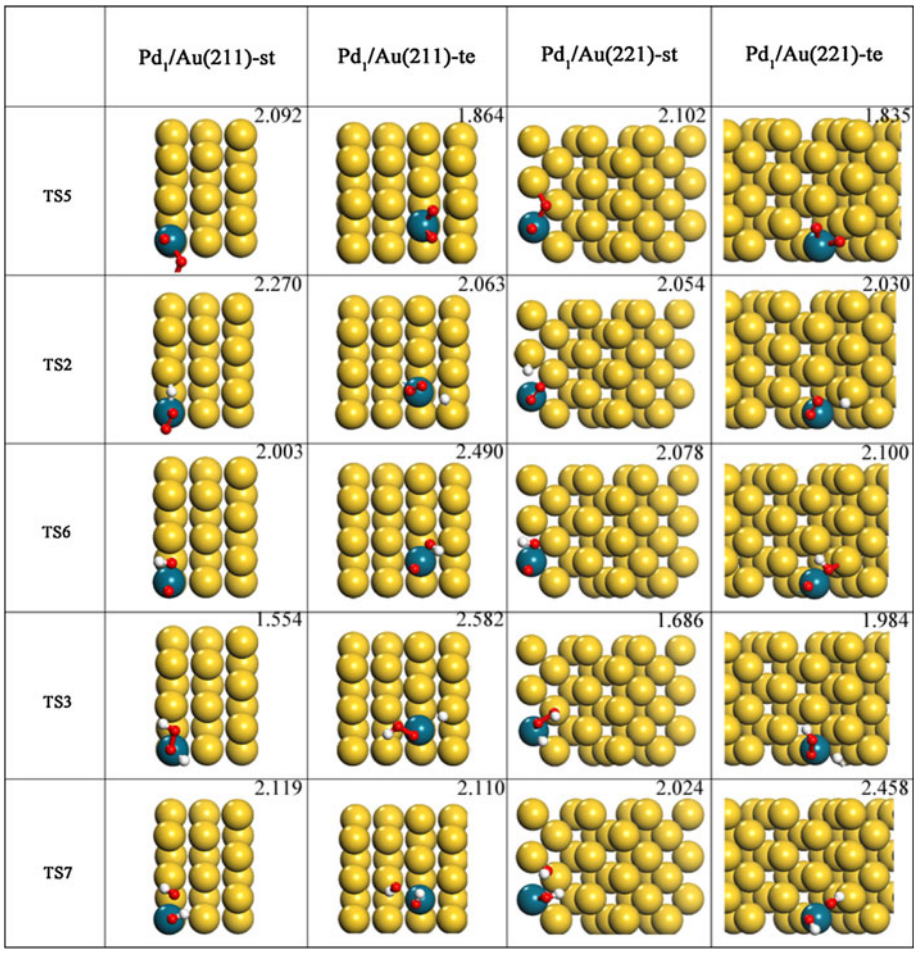

Fig. 5 The optimized transition states structures (*top view*) of the elementary steps on two stepped surfaces. The bond lengths are given in angstrom (Å)

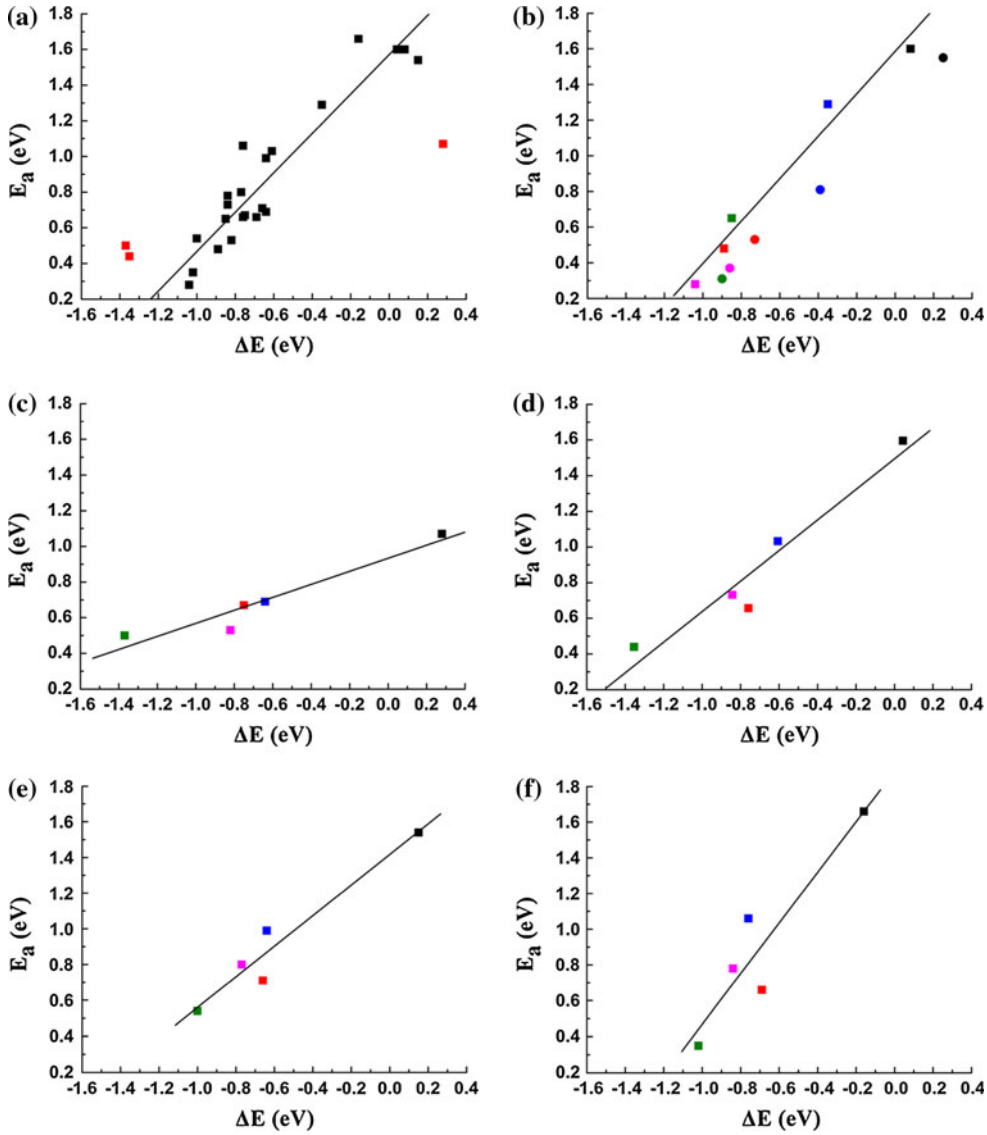

Fig. 6 The Brønsted–Evans–Polanyi relationship between the activation energies and reaction energies for a series of elementary reactions (*pink* indicates reaction (2); *red* indicates reaction (3), *black* indicates reaction (5), *blue* indicates reaction (6), *green* indicates reaction (7).). on **a** all the surfaces, the *red dot* represent the data which is not consistent with rules, **b** Pd_1/Au(111), part of the data (*rounded dot*) taken from the literature of Hwang [20], **c** Pd_1/Au(100), **d** Pd_1/Au(110), **e** Pd_1/Au(211)-st and **f** Pd_1/Au(221)-st surface

reaction networks, which involve multiple elementary steps. Figure 6 shows the Brønsted–Evans–Polanyi plots for the calculated activation energies as the function of the reaction energies of elementary reaction of H_2O_2 synthesis on Pd_1/Au surfaces. Firstly, it is seen that, the activation energies of five elementary steps for H_2O_2 synthesis have an excellent linear relation with their reaction energies on three flat and the step sites of two stepped surfaces for both O–O bond dissociation and O–H bond formation. In fact, Au nanoparticles are mainly composed of Au(111) and Au(100) facets and a great number of steps. Therefore, the Brønsted–Evans–Polanyi relations for H_2O_2 synthesis identified in this study provide a simple descriptor for not only Au surfaces but also Au nanoparticles. Secondly, although the slop of the Brønsted–Evans–Polanyi relations is close to one (Fig. 6a), which originate from the transition states geometries are very similar with the final state ones (as shown in Figs. 2, 5). The specific values of the relations are dependent on the surfaces (Fig. 6b–g). It indicates that the facet of catalysts nanoparticles is an important factor to determine the performance of H_2O_2 synthesis. Thirdly, as shown in Fig. 6b–g, for all of the investigated surfaces, the most difficult step among five elementary reactions is the dissociation of O_2. However, for Pd_1/Au(110) and the step site of Pd_1/Au(211) and Pd_1/Au(221), the easiest step is the dissociation of H_2O_2, while for Pd_1/Au(111), the most facile step is the hydrogenation. The coordination number of Pd on Au(111) and Au(100) is 9 and 8, while on Au(110), and step edge of Au(221) and Au(211), the value is 7. It is seen that the larger coordination number of Pd, the larger (smaller) activation energies for the dissociation (hydrogenation) reactions. From this point, Pd_1/Au(111) is the better catalysts for H_2O_2 synthesis than other three surfaces. Finally, the activation energies are direct

proportion to the reaction energies for both the formation of H_2O_2 via the hydrogenation and the dissociation reactions of three key species (O_2, OOH and H_2O_2). An ideal catalyst for H_2O_2 synthesis should have low activation energies for the H_2O_2 formation and high activation energies for the dissociation reaction, which indicate that the dissociation reaction should be endothermic or slightly exothermic and the hydrogenation should be exothermic. Therefore, our study provides a simple descriptor to estimate the energy barriers based on the reaction energies for H_2O_2 synthesis on metal surfaces and probably nanoparticles.

4 Conclusions

In conclusion, by the detailed analysis on the elementary steps for H_2O_2 formation, we found that Pd_1/Au(111) is the most suitable surfaces among the investigated five different surfaces (Pd_1/Au(111), Pd_1/Au(100), Pd_1/Au(110), Pd_1/Au(221) and Pd_1/Au(211)). Especially, our study found that the activation energies of five elementary steps for H_2O_2 synthesis have an excellent linear relation with their reaction energies on three flat surfaces and the step edge sites of two stepped surfaces for both O–O bond dissociation and O–H bond formation, which are consistent with the Brønsted–Evans–Polanyi relations. This study provides a simple method to estimate the reaction barriers of elementary steps of H_2O_2 synthesis. This study of H_2O_2 synthesis on a series of Au surfaces is also helpful for the design the Au nanoparticles with high activity and selectivity of H_2O_2 in industrial/application catalysis fields.

Acknowledgments This study was supported by the National Natural Science Foundation of China (NSFC-21176221 and 20906081), Zhejiang Provincial Natural Science Foundation of China (ZJNSF-R4110345) and the New Century Excellent Talents in University Program.

References

1. Campos-Martin JM, Blanco-Brieva G, Fierro JLG (2006) Angew Chem Int Ed 45:6962
2. Samnata C (2008) Appl Catal A 350:133
3. Edwards JK, Carley AF, Herzing AA, Kielyb CJ, Hutchings GJ (2008) Faraday Discuss 138:225
4. Landon P, Collier PJ, Papworth AJ, Kiely CJ, Hutchings GJ (2002) Chem Commun 2058
5. Sinha AK, Seelan S, Tsubota S, Haruta M (2004) Angew Chem Int Ed 43:1546
6. Hughes MD, Xu YJ, Jenkins P, McMorn P, Landon P, Enache DI, Carley AF, Attard GA, Hutchings GJ, King F, Stitt EH, Johnston P, Griffin K, Kiely CJ (2005) Nature 437:1132
7. Abad A, Conception P, Corma A, Garcia H (2005) Angew Chem Int Ed 44:4066
8. Corma A, Serna P (2006) Science 313:332
9. Wang JG, Hammer B (2006) Phys Rev Lett 97:136107
10. Matthey D, Wang JG, Wendt S, Matthiesen J, Schaub R, Lægsgaard E, Hammer B, Besenbacher F (2007) Science 315:1692
11. Wang JG, Hammer B (2007) Top Catal 44:49
12. Abate S, Centi G, Melads S, Perathoner S, Pinna F, Strukul G (2005) Catal Today 104:323
13. Samnata C (2008) Appl Catal A 350:133–149
14. Edwards JK, Solsona B, Ntainjua NE, Carley AF, Herzing AA, Kiely CJ, Hutchings GJ (2009) Science 323:1037
15. Edwards JK, Ntainjua NE, Carley AF, Herzing AA, Kiely CJ, Hutchings GJ (2009) Angew Chem Int Ed 48:8512
16. Han YF, Zhong Z, Chen F, Chen L, White T, Tay Q, Yaakub SN, Wang ZJ (2007) J Phys Chem C 111:8410
17. Ishihara T, Hata Y, Nomura Y, Kaneko K, Matsumoto H (2007) Chem Lett 36:878
18. Mazzone G, Rivalta I, Russo N, Sicilia E (2009) Chem Commun 1852
19. Chen MS, Kumar D, Yi CW, Goodman DW (2005) Science 310:291
20. Ham HC, Hwang GS, Han J, Nam SW, Lim TH (2009) J Phys Chem C 113:12943
21. Jirkovsky JS, Panas I, Ahlberg E, Halasa M, Romani S, Schiffrin DJ (2011) J Am Chem Soc 133:19432
22. Kesavan L, Tiruvalam R, Rahim MHA, Saiman MI, Enache DI, Jenkins RL, Dimitratos N, Lopez-Sanchez JA, Taylor SH, Knight DW, Kiely CJ, Hutchings GJ (2011) Science 331:195
23. Ksar F, Ramos L, Keita B, Nadjo L, Beaunier P, Remita H (2009) Chem Mater 21:3677
24. Liu RH, Yu YC, Yoshida K, Li GM, Jiang HX, Zhang MH, Zhao FY, Fujita S, Arai M (2010) J Catal 269:191
25. Barton DG, Podkolzin S (2005) J Phys Chem B 109:2262
26. Kacprzak KA, Akola J, Hakkinen H (2009) Phys Chem Chem Phys 11:6359
27. Todorovic R, Meyer RJ (2011) Catal Today 160:242
28. Staykov A, Kamachi T, Ishihara T, Yoshizawa K (2008) J Phys Chem C 112:19501
29. Ham HC, Hwang GS, Han J, Nam SW, Lim TH (2010) J Phys Chem C 114:14922
30. Ham HC, Stephens JA, Hwang GS, Han J, Nam SW, Lim TH (2011) Catal Today 165:138
31. Li J, Staykov A, Kamachi T, Ishihara T, Yoshizawa K (2011) J Phys Chem C 115:7392
32. Barrio L, Liu P, Rodriguez JA, Campos-Martin JM, Fierro JLG (2007) J Phys Chem C 111:19001
33. Brønsted N (1928) Chem Rev 5:231
34. Evans MG, Polanyi NP (1938) Trans Faraday Soc 34:11
35. Delley B (1990) J Chem Phys 92:508
36. Delley B (2000) J Chem Phys 113:7756
37. Hammer B, Hansen LB, Nørskov JK (1999) Phys Rev B 59:7413
38. Govind N, Petersen M, Fitzgerald G, King-Smith D, Andzelm J (2003) Comp Mater Sci 28:250
39. Henkelman G, Uberuaga BP, Jonsson H (2000) J Chem Phys 113:9901
40. Olsen RA, Kroes GJ, Henkelman G, Arnaldsson A, Jonsson H (2004) J Chem Phys 121:9776